J. Lorenzo, A. Lázaro, R. Villarino and D. Girbau. “Active Backscatter Transponder for FMCW Radar Applications”, IEEE Antennas and Wireless Propagation Letters, vol. 14, pp. 1610-1613, 2015.

doi: 10.1109/lawp.2015.2414295

URL: https://ieeexplore.ieee.org/document/7063261

Active Backscatter Transponder for FMCW Radar Applications

J. Lorenzo, A. Lazaro, *Member, IEEE*, R. Villarino and D. Girbau, *SeniorMember, IEEE*

***Abstract*— This paper presents a low-cost wideband active backscatter transponder at X-band suitable for Frequency-modulated continuous-wave (FMCW) radar applications. In order to maximize its read range, the radar cross section (RCS) of the transponder is increased by means of a two-stage amplifier based on High Electron Mobility Transistors (HEMT), which is connected between two (one receiver and one transmitter) bowtie antennas. To distinguish the transponder response from stationary clutter it modulates the level of its RCS modifying the bias of the transistors. The backscattered response of the transponder is collected using a FMCW commercial radar. The transponder achieves a bandwidth of 7-12 GHz, with a gain between 18-22 dB, and a power consumption of 75 mW. Theoretical operation and experimental results are presented.**

***Index Terms*—FMCW radar, transponder, RFID.**

I. Introduction

FMCW radar transmits a signal that is usually swept linearly in frequency. Low-cost FMCW radars often use homodyne receivers. In these receivers, reflections from the objects are mixed with the transmitted signal to produce a beat signal (low-pas filtered signal at the output of the mixer) whose frequency is proportional to the distance between the radar and the target [1]. FMCW radars are commonly used in several applications such as altimeters or tank levels where high-resolution non-contact measurements in harsh conditions are required [2]. In recent years, FMCW radar has also been used as reader for long-distance transponders integrating different types of sensors such as pressure [3] or temperature sensors [4].

One of the problems to detect the target is the clutter contamination derived from multipath reflections [5]. This is of major concern when the target radar cross section (RCS) is smaller than that of other surrounding objects. In order to mitigate this problem, a modulated backscatter transponder has been proposed in [6]. In this case the spectrum at the output of the mixer is shifted by the modulated frequency of the tag, f_{tag}. The range measurement using FMCW radar is performed by analyzing the spectrum of the beat signal around f_{tag} and by verifying the presence of a couple of peaks. The frequency difference between peaks is proportional to the distance between the radar and the tag. The read range using passive backscatter transponder system such as [6] is about 10 m with a transmit power of 10 dBm. One method to increase the read range from tens to hundreds of meters has been proposed in [7] using switched injection-locked oscillator (SILO) transponders at 5.8 GHz ISM band, with the die micrograph of the reflector circuit [8]. But the complexity and power consumption of the tag is higher than in passive backscatter modulation schemes based on a backscattering antenna. An alternative approach based on active Van Atta arrays has also been investigated [9-12]. A design at 5.8 GHz ISM band that combines the injection locking technique and retrodirective active Van Atta arrays has been proposed in [10]. An improvement consists of the utilization of active Van Atta arrays with the receiver and transmitter antennas placed in cross polarization to reduce coupling and avoid oscillations. However the complexity of the system is greater and the use of several amplifiers increases the power consumption. In order to improve measurement precision, more sophisticated solution based on switched injection-locked oscillator (SILO) tags that work at 34.45 GHz has been presented in [13].

It is known that the radar resolution depends on the bandwidth. Thus, another challenge is to increase the bandwidth in the former solutions. The retrodirective techniques are often narrowband designs [11]. In addition, the power consumption of an RF oscillator in secondary radars and of active Van Atta arrays is high, and the designs are complex and expensive. The high RCS can be achieved modulating high-gain antennas but then the tag needs to be oriented to the reader. In previous works, modulated frequency selective surfaces (FSS) are used to increase the differential RCS in transponders used for time-domain UWB [14] and in FMCW [15] radar applications. In these cases, the differential RCS increases with the number of FSS elements with a small power consumption, but also increases the directivity of the transponder. An active transponder for time-domain UWB RFID applications has been presented in [16] achieving long-range and using cross-polarization.

The aim of this work is to study the feasibility to use wide-band backscatter active transponders including a two-stage amplifier and low-gain decoupled wideband antennas. To this end, this paper presents the design and feasibility study of a X-band modulated active transponder read using a FMCW radar. The main features of the proposed design are: its wideband frequency response, it is lower cost and power consumption compared to other active solutions such as injection-locked or

Manuscript received June 16, 2014. This work was supported by the Spanish Government Project TEC2011-28357-C02-01 and BES-2012-053980.
J. Lorenzo, A. Lazaro, D. Girbau and R. Villarino are with the Electronics, Electrical and Automatics Engineering Department, Universitat Rovira i Virgili, 43007 Tarragona, Spain (antonioramon.lazaro@urv.cat, phone: +34-977.55.86.68).

Van Atta arrays. The prototype can be designed to operate at other bands by scaling dimensions of the bowtie antenna and by redesigning the amplifier at the new frequency band. The paper is organized as follows. Section 2 deals about the basic theory of the backscattered transponder and describes a transponder designed as a proof of concept. Experimental results are described in Section 3. Section 4 provides the conclusions.

II. MODULATED TRANSPONDER OPERATION AND DESIGN

A. Operation theory

Fig. 1 shows a block diagram of the proposed system composed by the FMCW radar and the transponder. The radar interrogates the transponder and it answers modulating its RCS. The transponder consists of two bowtie antennas interconnected by an amplifier whose bias current is controlled by an oscillator and is used to modulate the backscattered signal.

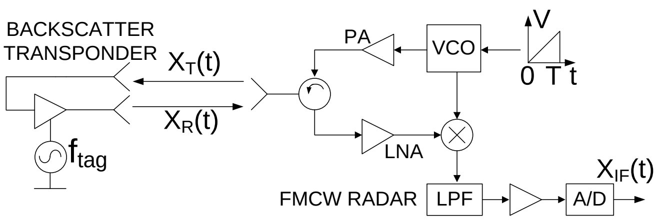

Fig. 1. Block diagram of the system.

Assuming that the frequency of the transmitted signal $x_T(t)$ is swept linearly, it can be written as:

$$x_T(t) = A\cos\left(2\pi(f_c t + \frac{1}{2}\mu t^2)\right) \tag{1}$$

where A is the amplitude, f_c is the carrier frequency, $\mu=B/T$, T and B are the sweep slope, duration and bandwidth respectively. The backscattered received signal $x_R(t)$ is the transmitted signal delayed by the round-trip time of flight (τ), attenuated and modulated at frequency f_{tag} (frequency of the oscillator).

$$x_R(t) = A'\cos\left(2\pi\left(f_c(t-\tau)+\frac{1}{2}\mu/t-\tau)^2\right)\right)\cos(2\pi f_{tag}t)$$

(2)

where $\tau=2d/c$, d is the transmitter to transponder distance, c is the speed of light and A' is the received amplitude. Assuming a simple homodyne receiver, the baseband signal is obtained from the output of the receiver mixer after it is low pass filtered. The baseband spectrum is schematically shown in Fig. 2.

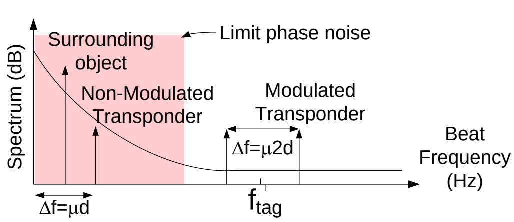

Fig. 2. Baseband spectrum using non-modulated and modulated transponders, in the presence of a parasitic reflector in the vicinity of the transponder.

Two cases are considered. The first case addresses a non-modulated transponder. Here the distance is obtained using the FMCW radar equation and the transponder is difficult to be detected due to the phase noise and because it might be interfered by the reflections at surrounding objects with higher RCS (e.g. metallic objects). The second case addresses a modulated transponder. Here the target can be detected from a couple of peaks around f_{tag} and the distance can be obtained from the frequency separation (Δf) between them, which is proportional to the distance [15].

$$\Delta f = \mu\tau = \mu 2d/c \rightarrow d = c\Delta f/(2\mu) \tag{3}$$

In the latter, the transponder can be more easily read since interferences have smaller amplitude and detection is not limited by phase noise but by the receiver noise figure.

B. Transponder design

A transponder is manufactured as a proof-of-concept on Rogers 4003 substrate (relative permittivity ε_r=3.54, loss tangent tanδ=0.003, and height 32 mil). The transponder operates between 9.25 GHz and 10.75 GHz, because it is the frequency band of the FMCW radar used as reader (Siversima model RS3400X). The control of the coupling or the isolation is performed by modifying the distance between two antennas. Also in order to achieve the bandwidth requirements, two wideband bowtie dipole antennas [17], designed with ADS/Momentum are integrated in the transponder (see the inset in Fig.3). The length of the arms is 6.6 mm and the angle is 70 degrees. A balun is used to convert the balanced feed line into a 50 Ω microstrip line. It is implemented in a similar way to [17] but a 13.5 mm tapered microstrip line is used instead of a quarter wavelength transformer. A metallic reflector is located at 7 mm to increase the gain. The simulated reflection coefficient and gain are shown in Fig. 3.

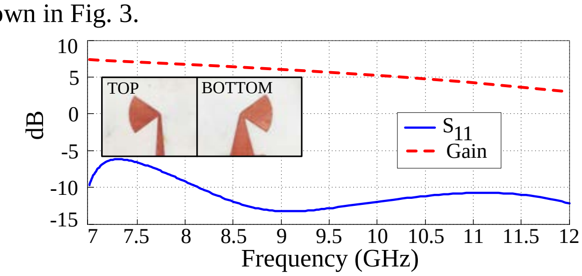

Fig. 3. Simulated reflection coefficient (S_{11}) and antenna gain.

Fig. 4 a-b show the electrical schematic and photography of a two-stage amplifier based on CEL NE3503M04 HEMT transistors, that is placed between transmitter and receiver antennas. A schematic circuit of the modulating oscillator and current driver is shown in Fig.4.c. A low power oscillator is based on a ICM555 that only draws 60 µA from a 3 V DC supply. The total current consumption of the transponder is 25 mA from 3 V DC supply, and it is less compared to proposed systems [8], [10], [13]. Fig. 5 shows the measured S parameters of the amplifier for V_G=-0.3V and V_D=2.5V, I_D=25 mA using a board with SMA connectors. The difference between the measured S_{22} response and the simulations has been observed due to the parasitics of the stabilization resistances which are welded to the drain of the transistors. These resistances are used to reduce the gain at low frequency and to avoid the oscillation of the transceiver. The stability of the amplifier on the entire frequency band was tested after analyzing stability factor is greater than unity. A key point in the design of this transponder is to minimize the coupling between antennas. Fig. 6 shows the open-loop gain computed from the cascade simulation of the antennas coupling with and without amplifier. It can be seen that the coupling between antennas is enough small to avoid oscillation. The wake-up process of the transponder is not addressed in this paper, but must be taken into account to optimize the battery lifetime. A wake-up circuit similar to the one described in [14] could be used.

The amplitude of the modulated reflected signal depends on the RCS of the active transponder σ, given by [18]:

$$\sigma = \frac{\lambda^2}{4\pi} G_{tag,r} G_a G_{tag,t} \tag{4}$$

where λ is the wavelength, $G_{tag,r}$,$G_{tag,t}$ are the transponder receiver and transmitter antenna gains, respectively, and G_a is the amplifier gain. Fig. 7 shows the computed RCS using (4). A large enhancement due to amplifier gain can be observed from 7 to 12 GHz.

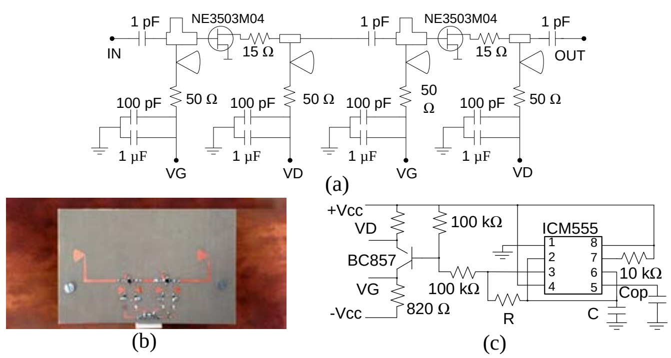

Fig. 4. (a) Circuit schematic of the two-stage amplifier, (b) photograph of the transponder (top view) and the ground reflector and (c) circuit schematic of the oscillator.

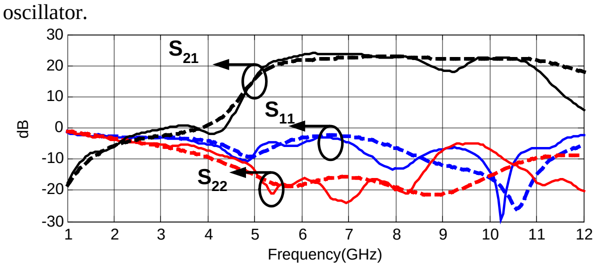

Fig. 5. Measurements (solid line) and simulations (dotted line) of S_{11}, S_{22} and S_{21} parameters of the two-stage amplifier.

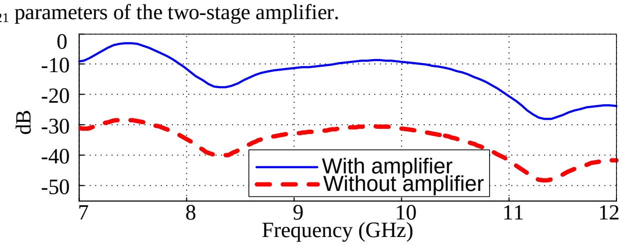

Fig. 6. Simulated open-loop gain without amplifier (dotted line) and with amplifier (solid line).

III. Experimental Results

Measurements in outdoor environment between 3 and 18 m are performed using commercial radar RS3400X from Siversima. It is a synthesized X-band FMCW radar front-end. The nominal transmitted power is 0dBm±5dB. The radar sweeps the 9.25-10.75 GHz frequency band with sweep time of 75 ms and it is connected to a 20 dB standard pyramidal horn. Fig.8.a shows the measurement of the transponder at 8 m without modulation and Fig.8.b shows the measurement at the same distance but now modulated at 7 kHz. Here a background subtraction technique is applied, subtracting the measurement of Fig. 8.a (non-modulated). The peaks are clearly detected (black circles). A 90º rectangular dihedral reflector (20 cm by 29 cm) is located in the vicinity of the transponder. This reflector presents a high RCS (19.7 dB oriented to the radar). The peak of this reflector is also clearly observed in Fig. 8, which justifies the need for modulation.

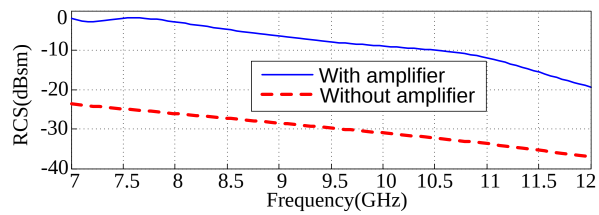

Fig. 7. Simulated RCS of the active transponder as a function of frequency with (solid line) and without (dotted line) the amplifier.

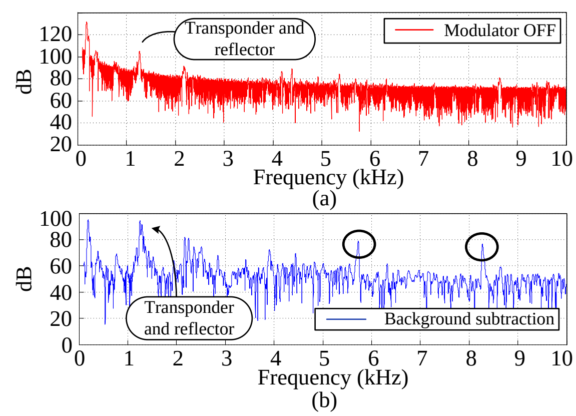

Fig. 8. Measurement of the transponder and dihedral reflector at 8 m (a) in case of no modulation or (b) with f_{tag}=7 kHz modulation.

Fig. 9 shows the sideband peaks obtained from the measurement of the modulated transponder at different distances (from 3.2 m to 13.5 m). The distances are derived from the spacing between the peaks and match with the measured distances between the radar and the transponder. Fig. 10.a shows the estimated distance obtained from the measurement of the transponder and from the dihedral reflector. The maximum non-ambiguous distance is limited by the sampling frequency (f_s) of the A/D converter used [15] (20 kHz for the Siversima controller card used in our case). Here, this distance corresponds to the case when the frequency of the second peak reaches the frequency $f_s/2$. Therefore the maximum non-ambiguous distance is given by $c(f_s/2-f_{tag})/(2\mu)$=22.5 m. Fig. 10.b shows the angular dependence of the normalized measured power at 9, 10 and 11 GHz. The measured 3-dB beamwidth in the H-plane is 80º at 10 GHz. The experimental setup described in Fig.11 is used to characterize the angular behavior of the transponder. A 20 dB standard horn antenna connected to a signal generator (Rohde SMF-100) is used to illuminate the transponder with a continuous wave. The receiver is composed by a horn antenna connected to a spectrum analyzer (Rohde FSP-30). Finally, in Table I there is a brief comparison between the proposed prototype and other active transponders in the literature.

TABLE I
COMPARISON WITH OTHER ACTIVE TRANSPONDERS

Ref.	Frequency Band (GHz)	EIRP (dBm)	Measured Range (m)	Power consumption
[8]	5.65	10	6.5 Res 18 cm	140 mW
[10]	5.65 (1 MHz locking range)	28	4.7	130 mW (t) 260mW (Van atta)
[13]	32.7-35.4	36	11.5 Res 7.5 cm	770 mW (t) 122mW (pulsed, only SILO)
This work	7-12 (t) 9.25-10.75(radar)	20-25	18 Res < 10 cm	75 mW

t: Transponder, Res: Resolution

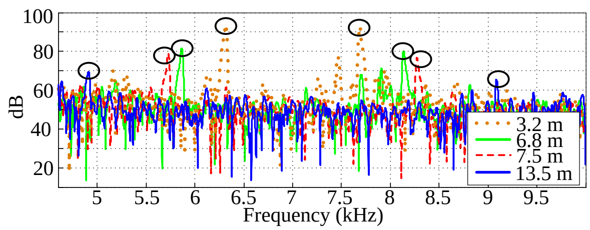

Fig. 9. Measurement of the modulated transponder with f_{tag}=7 kHz using the background subtraction technique.

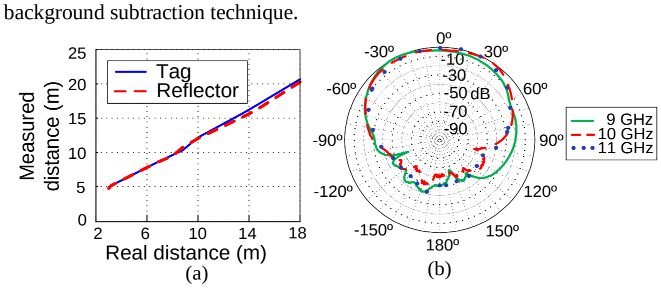

Fig. 10. (a) Measured distance obtained from the dihedral reflector (dashed line) and derived from the spacing between the sideband peaks (solid line). (b) Normalized measured power as function of angle at 9, 10 and 11 GHz.

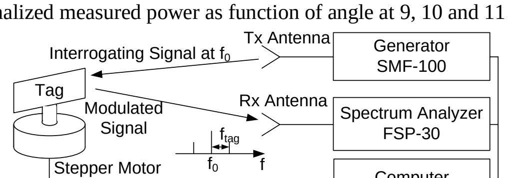

Fig. 11. Experimental setup used to measure the transponder angular response.

IV. CONCLUSION

This work has studied the feasibility of using a wideband (7-12 GHz) active backscattered modulated transponder based on a couple of bowtie antennas interconnected by a two-stage amplifier for FMCW radar applications. The basic operation theory of the system is explained. Since the RCS is modulated using an oscillator that drives the amplifier bias, interferences which come from stationary clutter can be removed using a simple background subtracting technique, which consists of subtracting the non-modulated from the modulated transponder measurements. Experimental results are obtained using commercial low-power X-band FMCW radar (9.25-10.75 GHz) working as a reader. The transponder has low production cost and its power consumption is lower than other systems presented in several works presented in literature, based on injection-locking oscillators or Van Atta arrays. The use of the amplifier allows detecting the transponder at distances up to 18 m, near the non-ambiguous distance of the system. An 80º angle in H-plane at 3-dB beamwidth is measured.

REFERENCES

[1] M.I. Skolnik, "Introduction to Radar Systems ," in *McGraw-Hill*, 2nd ed. Singapure, 1981.

[2] D. Brumbi, "Low power FMCW radar system for level gauging," in *IEEE MTT-S International Microwave Sysmposium Digest*, Boston, MA (USA), 2000, vol. 3, pp. *1559-1562*.

[3] H.Aubert, F.Chebila, M.Jatlaoui, T.Thai, H.Hallil, A.Traille, S.Bouaziz, A. Rifai, P.Pons, P.Menini, and M.Tentzeris, "Wireless sensing and identification of passive electromagnetic sensors based on milimetre-wave FMCW radar," *IEEE International Conf. on RFID-Technologies and Applications* (RFID-TA), Nice (France), 2012, pp. 398-403.

[4] P.Pons, H.Aubert, P.Menini, and M.Tentzeris, "Wireless Passive autonomous Sensors with Electromagnetic Transduction," *International Conference on Microwave and High Frequency Heating*, Toulouse (France), 2011.

[5] J.Thornton, and D.J.Edwards, "Range measurement using modulated retro-reflectors in FM radar system," *IEEE Microwave Guided Wave Lett.*, Vol. 10,pp. 380-382, 2000.

[6] M.Kossel, H.R.Benedickter, R.Peter, and W.Bächtold, "Microwave backscatter modulation systems," *IEEE Int. Microwave Symp. Dig.*, Boston, MA (USA), 2000, pp. 1427-1430.

[7] M.Vossiek, and P.Gulden, "The Switched Injection-Locked Oscillator: A Novel Versatile Concept for Wireless Transponder and Localization Systems," *IEEE Transactions on Microwave Theory and Techniques*, Vol.56, No.4,pp. 859-866, 2008.

[8] S.Wehrli, R.Gierlich, J.Hüttner, D.Barras, F.Ellinger, and H.Jäckel, "Integrated Active Pulsed Reflector for an Indoor Local Positioning System," *IEEE Transactions on Microwave Theory and Techniques*, Vol.58, No.2, pp.267-276, Feb 2010.

[9] G.Avitabile, A.Cidronali, G.Manes, G.B.Gentili, "An integrated active transponder for ISM-band applications," *Sixth International Conf. on Radio Receivers and Associated Systems*, pp.172-175, 26-27 Sep 1995.

[10] C.Luxey, and J.-M. Laheurte, "A retrodirective transponder with polarization duplexing for dedicated short-range communications," *IEEE Transactions on Microwave Theory and Techniques*, Vol.47, No.9, pp.1910-1915, Sep 1999.

[11] T.-J. Hong, and S.-J. Chung, "24 GHz active retrodirective antenna array," *Electronics Letters* , Vol.35, No.21, pp.1785-1786, 14 Oct 1999.

[12] S. J. Chung; S. M. Chen, and Y. C. Lee, "A novel bi-directional amplifier with applications in active Van Atta retrodirective arrays," *IEEE Transactions on Microwave Theory and Techniques*, vol. 51, pp. 542-547, Feb 2003.

[13] A.Strobel, C.Carlowitz, R.Wolf, F.Ellinger, andM.Vossiek, "A Millimeter-Wave Low-Power Active Backscatter Tag for FMCW Radar Systems," *IEEE Transactions on Microwave Theory and Techniques*, Vol.61, No.5, pp.1964-1972, May 2013.

[14] A.Lazaro, A.Ramos, D. Girbau, and R.Villarino, "A Novel UWB RFID Tag Using Active Frequency Selective Surface," IEEE Trans. on Antennas and Propagation, Vol.61, No.3, pp.1155-1165, March 2013.

[15] A.Lazaro, J.Lorenzo, R.Villarino, and D.Girbau, "Backscatter Transponder based on Frequency Selective Surface for FMCW Radar Applications," *Radioendineering*, Vol.23, No.2, pp. 632-641, June 2014.

[16] A.Lazaro, A.Ramos, R.Villarino, and D.Girbau, "Active UWB Reflector for RFID and Wireless Sensor Networks," in *IEEE Transactions on Antennas and Propagation*, Vol. 61, No. 9,pp. 4767-4774, 2013.

[17] G.Zheng, A.A.Kishk, A.W.Glisson, and A.B.Yakovlev, "A broadband printed bow‐tie antenna with a simplified balanced feed,"*Microwave and optical technology letters*, Vol.47, No.6, pp.534-536, 2005.

[18] D.R. Brunfeldt and F.T.Ulaby, "Active Reflector for Radar Calibration," *IEEE Trans. On Geoscience and Remote Sensing*, Vol.GE-22, No.2, pp.165-169,1984.